Available online at www.sciencedirect.com
SCIENCE DIRECT®
Bioorganic & Medicinal Chemistry Letters 15 (2005) 1675–1681
Bioorganic & Medicinal Chemistry Letters

Estrogen receptor ligands. Part 10: Chromanes: old scaffolds for new SERAMs

Qiang Tan,[a,*] Timothy A. Blizzard,[a] Jerry D. Morgan, II,[a] Elizabeth T. Birzin,[b] Wanda Chan,[b] Yi Tien Yang,[b] Lee-Yuh Pai,[b] Edward C. Hayes,[b] Carolyn A. DaSilva,[b] Sudha Warrier,[b] Joel Yudkovitz,[b] Hilary A. Wilkinson,[b] Nandini Sharma,[a] Paula M. D. Fitzgerald,[a] Susan Li,[a] Lawrence Colwell,[a] John E. Fisher,[b] Sharon Adamski,[b] Alfred A. Reszka,[b] Donald Kimmel,[b] Frank DiNinno,[a] Susan P. Rohrer,[b] Leonard P. Freedman,[b] James M. Schaeffer[b] and Milton L. Hammond[a]

[a]*Department of Medicinal Chemistry, Merck Research Laboratories, PO Box 2000, RY800-B107, Rahway, NJ 07065, USA*
[b]*Department of Molecular Endocrinology and Bone Biology, Merck Research Laboratories, PO Box 2000, Rahway, NJ 07065, USA*

Received 22 October 2004; revised 18 January 2005; accepted 19 January 2005

Abstract—The discovery, synthesis, and SAR of chromanes as ERα subtype selective ligands are described. X-ray studies revealed that the origin of the ERα-selectivity resulted from a C-4 *trans* methyl substitution to the *cis*-2,3-diphenyl-chromane platform. Selected compounds from this class demonstrated very potent in vivo antagonism of estradiol in an immature rat uterine weight assay, effectively inhibited ovariectomy-induced bone resorption in a 42 days treatment paradigm, and lowered serum cholesterol levels in ovx'd adult rat models. The best antagonists **8F** and **12F** also exhibited potent inhibition of MCF-7 cell growth and were shown to be estrogen receptor down-regulators (SERDs).

As part of an evolutionary program designed to exploit the chromane skeleton for the discovery of selective ligands for the estrogen receptors, we have recently reported our findings on the flavanone,[1] **I**, Z = CO, and dihydrobenzoxathiin,[2] **I**, Z = S, classes. The reports detailed the generation of ligands with a greater affinity for the α isoform of the estrogen receptor and were therefore labeled SERAMs, selective estrogen receptor alpha modulators. Of the two classes, the more potent dihydrobenzoxathiins, typically exhibited low to sub-nanomolar binding to ERα, with 50- to 100-fold selectivity, and as a result of further study, a derivative, **II**, was targeted for development as a potential agent for the treatment of osteoporosis. This report focuses on the further extension of this research and discloses the synthesis and biological properties of another new class of orally bioavailable SERAMs containing the parent chromane core structure **III**, wherein, the size and stereogenic placement of the substituent is crucial for both receptor potency and selectivity. This series of compounds contrasts our initial finding, wherein the unsubstituted chromane **III**, Y = OH, $R^1 = R^2 = H$, exhibited equipotent affinity for both ERα and ERβ.[1] In addition, the results of this study contrast the very early studies of the Central Drug Research Institute (India) in which similar 3,4-diaryl-chromanes were exploited as potential antifertility agents and led to the development of the nonsteroidal contraceptive agent centchroman **IV**,[3] and the more recent studies of the Novo Nordisk,[4] as NSERTs (nonsteroidal estrogen receptor therapeutics) or early SERMs. Further exploitation of the chromane scaffold has also provided non-subtype selective, potent chromenes **V**[5] and **VI**,[6] as SERMs of commercial interest. The series of compounds disclosed herein represent the first reported chromanes exhibiting ERα-selectivity (see Figures 1 and 2).

Keywords: Osteoporosis; Estrogen receptor; Chromane; Subtype selectivity; Estrogen receptor alpha; SERM; SERAM; Estrogen receptor antagonist; Cancer.
* Corresponding author. Tel.: +1 732 594 1276; fax: +1 732 594 9556; e-mail: qiang_tan@merck.com

0960-894X/$ - see front matter © 2005 Elsevier Ltd. All rights reserved.
doi:10.1016/j.bmcl.2005.01.046

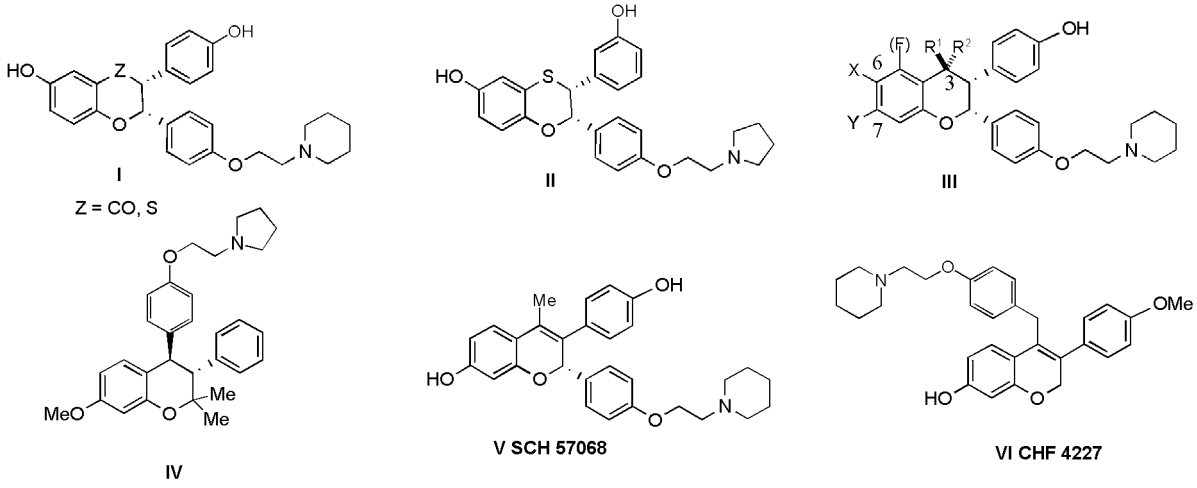

Figure 1.

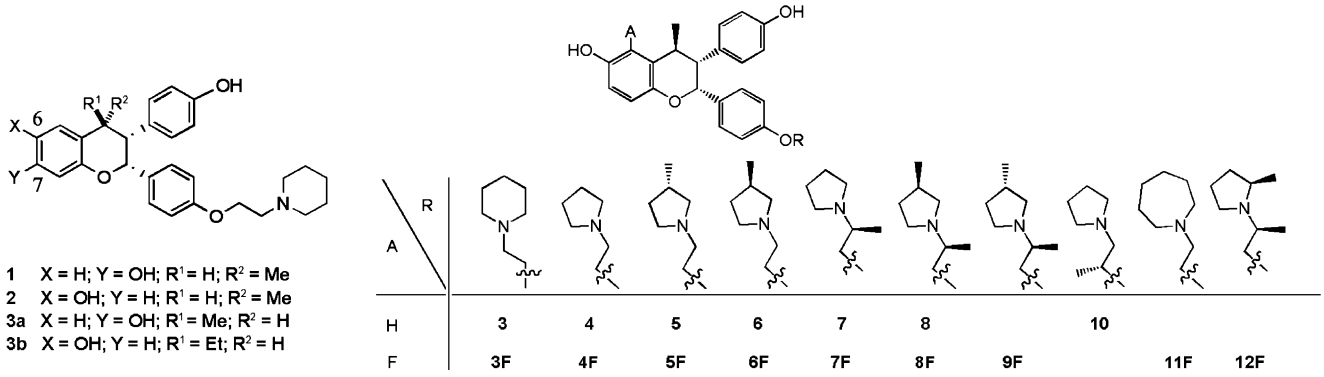

Figure 2. Novel chromanes **III**. **1**, **2**, and **3b** are racemic and the remainder are chiral.

The synthesis of the series **1**–**8**, **10**, **3a,** and **b** is depicted in Scheme 1 and featured diene **14**, which was obtained from the acid-induced elimination of the carbinol adduct formed by the addition of the Grignard reagent to coumarin **13**. Hydrogenation with Rh on carbon gave a mixture of alkenyl isomers **15** and **16**, in a ratio which averaged at 1:2.5. It was also found upon scale-up that the THP group was partially cleaved to give a mixture of protected and unprotected products. A second hydrogenation of **16** with Pd on carbon, with or without the THP group, provided chromanes **17** and **17a** (approximate ratio of **17**:**17a** = 1:1.4, R^1 = H; 1:4.5, R^1 = Me),

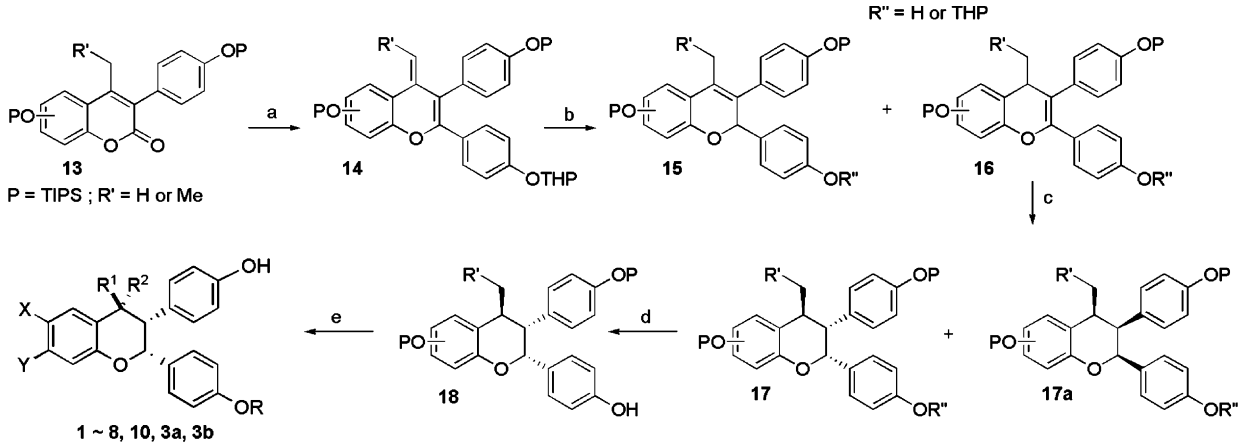

Scheme 1. Synthesis of **1**–**8**, **10**, **3a**, and **b**. Reagents and conditions: (a) (i) 4-(2-tetrahydro-2*H*-pyranoxy)phenylmagnesium bromide, THF, rt; (ii) 2 N anhydrous HCl in ether, 0 °C; (b) 1 atm H_2, EtOAc, 5% Rh–C, rt, ca 50% two steps; (c) 1 atm H_2, EtOAc, 10% Pd–C, rt; (d) (i) TFA, triethylsilane, CH_2Cl_2, 0 °C; skipped if THP is already completely removed in step c; (ii) chromatographic separation of isomers, ca 60% two steps; (e) (i) triphenylphosphine, DIAD, ROH, THF, rt; (ii) TBAF, THF, rt, ca 50%.

which upon treatment with TFA and subsequent chromatographic separation yielded **18**. In turn, **18** could be resolved by chiral HPLC. Finally, the installation of the aminoethyl side chain, by the use of a Mitsunobu reaction, in conjunction with protecting group manipulations, provided the target compounds.

The synthesis of the series of compounds possessing a C-5 fluorine substituent, **3F**–**9F**, **11F** and **12F**, is shown in Scheme 2. Selective ortho-lithiation with butyllithium via fluorine participation of the commercially available **19** followed by formylation with DMF gave rise to aldehyde **20**. After the selective demethylation of **20**, directed by complexation of $AlCl_3$ with the neighboring aldehyde functionality, the coupling of **21** with 4-methoxy phenylacetic acid yielded coumarin **22**. Following a protecting group switching maneuver, the DIBAL reduction of **24** provided the hemi-ketal **25**. This was followed by replacement of the hydroxyl group with the better phenoxyl leaving group, which in turn underwent a Grignard addition to yield **27**, according to the protocol by Grese and Pennington.[7] The *trans* methyl group was then installed by either of the two following methods. The first involved hydroboration followed by an oxidative work-up to provide for the installation of the hydroxyl group from the less hindered face of the less hindered carbon to yield **28**. Then under the influence of the nucleophilic, Lewis-acidic methyl titanium species, generated in situ from Me_2Zn and $TiCl_4$, the stereospecific delivery of the requisite methyl group was accomplished to provide **30**, presumably via the intermediacy of the benzylic cation (**a**) or its equivalent.[8] Alternatively, introduction of the *trans* methyl group was achieved by first converting **28** to iodide **29**, in an S_N1 manner, followed by treatment of the iodide with MeLi at low temperature. Presumably, fluorine-assisted metallation (**b**) of **28** generated lithium species **32** and MeI, which rapidly recombined to furnish **30**.

Finally, after removal of the benzyl protecting group, the aminoethyl side chains were installed as previously described using a Mitsunobu reaction protocol and the appropriate alcohol to generate final products after subsequent removal of the TIPS protecting groups.

As previously reported[2] by our laboratory, the dihydrobenzoxathiins **I**, Z = S exhibit ERα selectivity owing to the presence of a bulky sulfur atom which is tolerated by the nearby ERα-Leu384 residue but not by the ERβ-Met336 residue at the same position in the ligand binding domain of the receptor isoforms. By the same token, we suspected that a *cis*-methyl group at C-3 of the chromane system pointing toward the same residues should give rise to ERα selectivity. As depicted in Table 1, compounds such as **1** and **2** do exhibit ERα selectivity, however, with reduced binding affinity in comparison to **I**, Z = S. This may be attributed to the elevated steric congestion and hence the reduced conformational flexibility of the three *syn* substituents on the chromane ring. Indeed, when a *trans* methyl group was introduced, as in compounds **3** and **3a**, the ER binding affinity was dramatically improved. Truly surprising however, was the ERα selectivity found for **3** and **3a**, since a *trans* methyl group was not predicted to have a direct impact on selectivity.

A possible explanation for the observed selectivity was offered by the X-ray crystallography analysis[13] of the ERα complexes of these ligands. The structure of **4** in ERα (Fig. 3) revealed that although the *trans* methyl

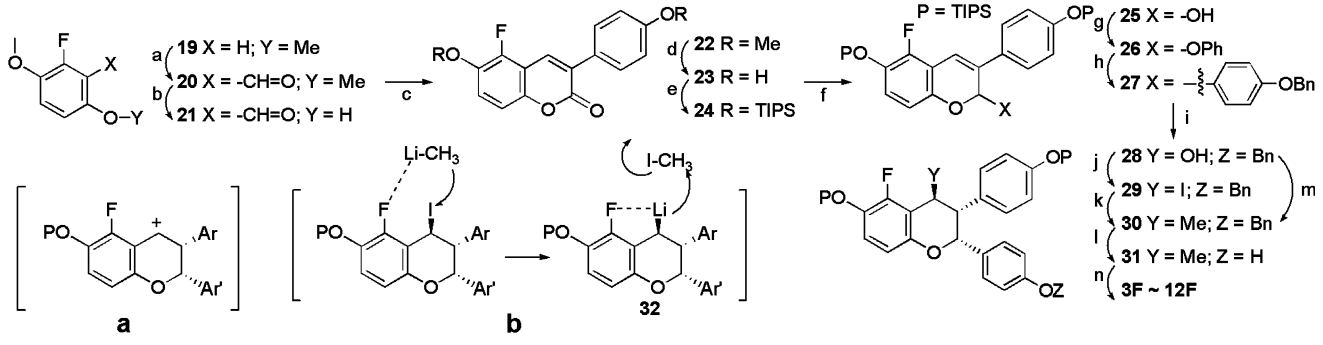

Scheme 2. Synthesis of **3F**–**7F**. Reagents and conditions: (a) BuLi, then DMF, THF, dry ice–acetone bath, 56%; (b) $AlCl_3$, CH_2Cl_2, rt, 84%; (c) 4-methoxyphenyl acetic acid, acetic anhydride, triethylamine, 135 ~ 145 °C, ca 50%; (d) BBr_3, CH_2Cl_2, 0 °C, 71%; (e) TIPSCl, Hunig's base, DMF, rt; (f) DIBAL, CH_2Cl_2, dry ice–acetone bath; (g) PhOH, CH_2Cl_2, rt; (h) 4-benzyloxyphenylmagnesium bromide, THF–toluene, 50 °C, 34% four steps; (i) Borane–THF complex, THF, rt, then 30% H_2O_2-aq Na_2CO_3, 82%; (j) KI, Bu_4NI, BF_3 etherate, CH_2Cl_2, 0 °C, 74%; (k) MeLi, THF, dry ice–acetone bath; (l) 1 atm H_2, EtOAc, 10% Pd–C, rt; 67% two steps; then chiral HPLC resolution; (m) Me_2Zn, $TiCl_4$, CH_2Cl_2, 51% two steps; (n) (i) triphenylphosphine, DIAD, ROH, THF, rt; (ii) TBAF, THF, rt, ca 50%.

Table 1. Binding affinity—IC_{50} (nM)[a]

Compd	1	2	3	3a	3b
ERα/ERβ (α-selectivity)	45/179(4)	38/627(17)	1.4/39(28)	0.66/13(20)	14/171(12)

[a] The single IC_{50} values were generated in an estrogen receptor ligand binding assay. This scintillation proximity assay was conducted in NEN Basic Flashplates using tritiated estradiol and full length recombinant human ER-alpha and ER-beta proteins, with an incubation time of 3 h. In our experience, this assay provides IC_{50} values that are reproducible to within a factor of 2–3.

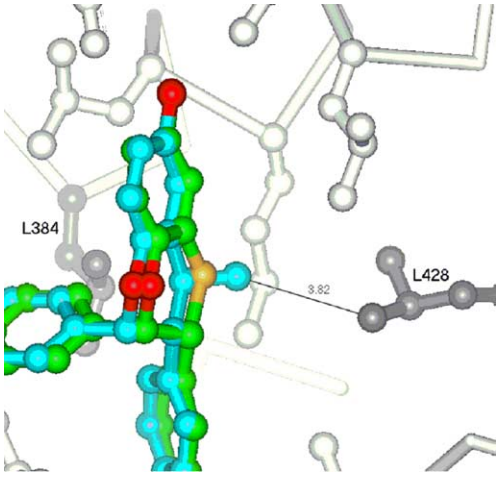

Figure 3. Comparison of the structures of **4** (cyan) and **I**, Z = S (green). The alpha carbons of the two proteins were aligned, and then the coordinates of **4** were added to the structure of **I**, where Z = S. The two residues that differ in sequence between ERα and ERβ are labelled. Oxygen atoms are colored red, and sulfur gold. The positions of the hydroxyl group are identical, but the added methyl group of **4** forces the compound to the left in this view, interacting more closely with L384, an interaction that would not be accommodated by the bulkier M336 of ERβ.

group indeed pointed away from the ERα-Leu384/ERβ-Met336 region, the addition of the methyl group forced the ligand to bind closer to this region in order to relieve a steric clash between the ligand methyl group and the side chain of L428. Therefore, the steric repulsion was elevated between that region of the receptor and the entire ligand, which then tended to mimic the effect of the bulky sulfur atom of the dihydrobenzoxathiin system. This also implied that the binding space in this region is probably very tight and thus the slightly larger ethyl analog **3b** exhibited dramatically lower binding affinity.

As shown in Table 2, several *trans* methyl chromane derivatives were evaluated for their ability (IC_{50}) to inhibit the estrogen dependent growth of both human carcinoma MCF-7 cells and an immature rat uterus, as well as, to lower serum cholesterol levels in OVX'd rats. As can be seen, all of the derivatives exhibited potent ERα affinity, with selectivity as high as 50–100-fold, and, unlike the dihydrobenzoxathiin class, which suffered a significant reduction in ERα selectivity upon incorporation of a fluorine atom on the aromatic ring,[2d] the corresponding fluorochromanes were found to be equally selective. Such an observation may further support the unique mechanism of selectivity proposed for chromanes which is based on the steric repulsion between the

Table 2. Binding affinity[a] and biological properties of compounds **3–7F**

Compd	IC_{50} (nM) ERα/ERβ (α-selectivity)	MCF-7 inhibition[b] IC_{50} (nM)	Uterine weight[c] %inhibition/%control @ 1 mpk	% Serum cholesterol reduction[d] (relative to raloxifene)
I(Z = S)	0.8/45 (56)[e]	3.0	99/9	—
3	1.4/39(28)	1.6	58/42	38(1.0)
3F	0.8/18(23)	1.4	65/26	45(1.2)
4	1.5/12(8)	1.5	5/24[f]	—
4F	0.9/11(12)	—	35/53	38(1.1)
5	1.3/19(15)	1.5	—	30(0.97)
5F	0.8/16(20)	0.9	47/54	42(1.2)
6	2.4/15(6)	1.2	68/31[f]	20(0.59)
6F	0.8/23(29)	1.1	84/2	27(0.9)
7	1.4/4.5(32)	0.5	67/30[f]	36(1.1)
7F	0.5/29(58)	0.5	85/1	29(0.97)
8	1.3/21(16)	0.4	7/20[f]	—
8F	0.9/26(29)	0.8	112/3	28(0.93)
9F	2.5/19(8)	0.6	75/23	31(0.97)
10	1.5/143(95)	2.5	—	—
11F	0.3/18(60)	0.9	41/53	17(0.57)
12F	0.7/4.1(6)	0.07	124/−13	—
Estradiol	1.3/1.1(1)[g]	—	—/100	86[h]

[a] The single IC_{50} values were generated in an estrogen receptor ligand binding assay. This scintillation proximity assay was conducted in NEN Basic Flashplates using tritiated estradiol and full length recombinant human ER-alpha and ER-beta proteins, with an incubation time of 3 h. In our experience, this assay provides IC_{50} values that are reproducible to within a factor of 2–3.

[b] Estrogen depleted MCF-7 cells were plated into 96-well cell culture plates at a density of 1000 cells/well. The test compounds and 3 pmol estradiol were applied to the cells on days 1 and 4 in order to evaluate the antagonist activity of compounds. The IC_{50} value was determined from the cellular protein content/well on day 9 of the assay.

[c] Twenty-day old intact female Sprague–Dawley rats were treated (po) with test compounds for 3 days at 1 mpk. The uteri wet weights were determined on day 4 and dry weights were determined after air-drying the tissue samples for 3 days. The anti-estrogenic (antagonism) activity of compounds was determined by co-administration of the compound with a subcutaneous injection of 17-beta-estradiol at 0.004 mpk and reported as % inhibition of uterine growth induced by estradiol. The estrogenic activity (partial agonism) of the compounds was determined by administering the test compound without estradiol and reported as % control.

[d] In ovx'd rats dosed at 1.5 mg/kg/day, po, for 3 days.

[e] Average of 36 measurements.

[f] Subcutaneous dosing @ 1 mpk.

[g] Average of 130 measurements.

[h] Average of 15 measurements at 0.6 mpk.

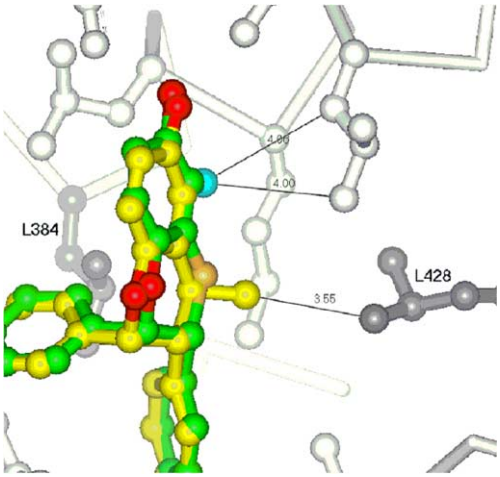

Figure 4. Comparison of the structures of **3F** (yellow) and **I**, Z = S (green). The alpha carbons of the two proteins were aligned, and then the coordinates of **3F** were added to the structure of **I**, Z = S. The two residues that differ in sequence between ERα and ERβ are labelled. Oxygen atoms in the ligands are colored red, sulfur gold, and fluorine cyan. Unlike the comparison of **4** and **I**, Z = S, the hydroxyl groups of these two compounds do not occupy identical positions. Rather, the addition of the fluorine atom forces **3F** down in this view, a repositioning that is combined with the move to the left generated by the addition of the methyl group.

receptor and the entire ligand (Fig. 4), wherein, the fluorine substituent enhances the bulkiness of the ligand. In contrast, the decrease in the selectivity of the fluorodihydrobenzoxathiins may arise from a reduction of the electron density on sulfur, and in turn, a reduction of the electronic repulsion with the Met366 residue of ERβ.

The introduction of the fluorine substituent on the chromane skeleton also appeared to improve the in vivo properties of the class, as evidenced by a comparison of the results from the uterine weight and serum cholesterol assays performed in rats, with those of the unsubstituted versions, in which selected basic side-chains were varied. It also became apparent that the nature of the side chain also produced more dramatic effects on the antagonism of estradiol in the uterine weight model with the chromane derived compounds than the corresponding dihydrobenzoxathiins. For example, the difference in the activities for the piperidine based compounds, **3** and **3F**, with those of the corresponding pyrrolidine based compounds, **4** and **4F** is most profound. On the other hand, the identical comparison found little or no difference with dihydrobenzoxathiins.[2b] Similarly, the differences observed between **5F** and **6F** were far less remarkable in the latter class. (The uterine weight %inhibition/%control @ 1 mpk, for dihydrobenzoxathiins corresponding to **3**, **3F**, **4**, **4F**, **5F** and **6F** are: 99/9, 102/1, 72/34, 79/19, 91/14, and 106/0, respectively.)

In addition, all compounds exhibited potent inhibition of the growth of MCF-7 tumor cells and the best antagonists, **8F** and **12F**, bearing side chains known to effect the stability of the ERα protein in the dihydrobenzoxathiin class of ER ligands,[9] were also shown to destabilize the protein in MCF 7 cells[10] to a comparable extent as the selective estrogen receptor down-regulator (SERD) Fulvestrant[11] (Fig. 5). This is in direct contrast to Tamoxifen which increased the ER protein level. Thus, chromanes such as **12F**, like their dihydrobenzoxathiin counterparts, may offer the potential to provide an alternative means for the treatment of estrogen-sensitive and Tamoxifen-resistant breast cancers.

Table 3 depicts the pharmacokinetic properties exhibited for a representative number of compounds in the chromane class as determined in female Sprague–Dawley rats. Reminiscent of our findings[2d] in the dihydrobenzoxathiin class of SERAMs, the disposition of the hydroxyl group on the chromane skeleton was crucial for good oral bioavailability. Thus, the C-7 positioned phenol, **3a**, exhibited very poor oral absorption, whereas, the analogous C-6 positioned phenol, **3**, had significantly improved absorption. As previously delineated,[2d] the Rosati model[12] and the subtilis present in dihydrobenzoxathiins appear to be inherent in the chromane system as well. Although, the addition of the fluorine atom did not appear to further affect oral

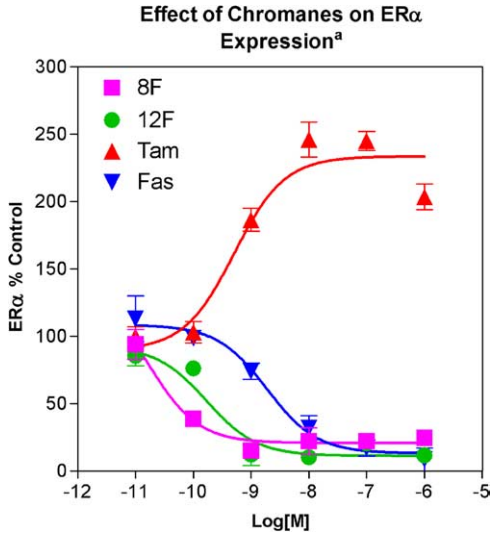

Figure 5. Effect of chromanes on ERα expression: MCF-7 cells were grown in an estrogen deprived medium for 48 h followed by exposure to the test compounds at various concentrations for 24 h. The cells were fixed and immuno-stained for ERα and visualized by fluorescence conjugated secondary antibody. ERα specific immuno-fluorescence was quantitated using Arrayscan Technology (Cellomics). Dose titrations were performed and the EC50s of destabilization as well as equilibrium levels of ERα attained were calculated. Tam = tamoxifen. Fas = Faslodex (Fulvestrant).

Table 3. Pharmacokinetics[a] of selected chromanes

Compd	**3**	**3F**	**3a**	**6F**	**7F**	**9F**
Clp (mL/min/kg)	7.7	16.9	9.5	17.8	42.6	9.0
$t_{1/2}$ (h)	8.1	11.2	5.9	8.0	4.4	16.1
F%	45%	54%	**2%**	43%	31%	44%

[a] Mean plasma concentrations and pharmacokinetic parameters in female, Sprague–Dawley rats following intravenous dosing at 1 mpk ($n = 2$) and oral dosing at 2 mpk ($n = 3$).

Table 4. Six-week bone mineral density study: adult OVX rats[a]

Compd		% Cholesterol reduction	% Uterine growth	Bone mineral density (% repleted to sham)	
				Distal femur:central	DFM:central
0.15, 0.5, 1.5 mpk	**3F**[b]	15,31,39	16,16,18	—	55,—,56
	6F	37,39,33	24,34,24	—,78,—	—,76,—
	7F	39,55,55	26,31,34	52,86,60	55,100,65
	9F	46,46,47	36,25,34	56,87,48	57,73,56
1.5 mpk	Raloxifene	49	30	74	64

[a] Six month old rats were ovariectomized (OVX) and treated with vehicle, ethinyl estradiol (EE; 0.6 mg/kg/day, po) or compound for 6 weeks. At the end of treatment, rats were necropsied and uterine weights measured. Femora were extracted and stored in 70% ethanol. Soft tissue was dissected from the bone, and bone mineral density (BMD) was measured by dual energy X-ray absorptiometry at both the distal femoral metaphysis (DFM) and the central femur. To compensate for differences in bone size between animals, results are expressed as the distal to central ratio.
[b] Raloxifene was not included as control in the assay.

bioavailability, it did appear to extend the serum half-life of **3F**.

In order to complete the evaluation of the chromane class as SERMs, several representative derivatives underwent evaluation to inhibit ovariectomized induced bone resorption in a six-week oral treatment paradigm in rats. As shown in Table 4, all of the chromane derivatives were found to possess raloxifene-like activity on serum cholesterol and bone mineral density.

In conclusion, given the profile of activity displayed by the new, highly substituted chromanes, this novel class qualifies as new SERAMs which may warrant further investigation.

Acknowledgements

The authors would like to thank Dr. Mats Carlquist and his colleagues at Karo-Bio for providing protein samples for X-ray crystallography analysis. Use of the Advanced Photon Source beamline 17-ID was supported by the companies of the Industrial Macromolecular Crystallography Association through a contract with Illinois Institute of Technology.

References and notes

1. Chen, H. Y.; Dykstra, K. D.; Birzin, E. T.; Frisch, K.; Chan, Y.; Yang, Y.; Mosley, R. T.; DiNinno, F.; Rohrer, S. P.; Schaeffer, J. M.; Hammond, M. L. *Bioorg. Med. Chem. Lett.* **2004**, *14*, 1417.
2. (a) Kim, S.; Wu, J. Y.; Birzin, E. T.; Frisch, K.; Chan, W.; Pai, L.-Y.; Yang, Y. T.; Mosley, R. T.; Fitzgerald, P. M. D.; Sharma, N.; Dahllund, J.; Thorsell, A.-G.; DiNinno, F.; Rohrer, S. P.; Schaeffer, J. M.; Hammond, M. L. *J. Med. Chem.* **2004**, *47*, 2171; (b) Chen, H. Y.; Kim, S.; Wu, J. Y.; Birzin, E. T.; Chan, W.; Yang, Y. T.; DiNinno, F.; Rohrer, S. P.; Schaeffer, J. M.; Hammond, M. L. *Bioorg. Med. Chem. Lett.* **2004**, *14*, 2551; (c) DiNinno, F. P.; Chen, H. Y.; Kim, S.; Wu, J. Y. International Patent WO200232377; (d) Kim, S.; Wu, J. Y.; Chen, H. Y.; Birzin, E. T.; Chan, W.; Yang, Y. T.; Colwell, L.; Li, S.; Dahllund, J.; DiNinno, F.; Rohrer, S. P.; Schaeffer, J. M.; Hammond, M. L. *Bioorg. Med. Chem. Lett.* **2004**, *14*, 2741; (e) Tan, Q.; Birzin, E. T.; Chan, W.; Yang, Y. T.; Pai, L. Y.; Hayes, E. C.; DaSilva, C. A.; DiNinno, F.; Rohrer, S. P.; Schaeffer, J. M.; Hammond, M. L. *Bioorg. Med. Chem. Lett.* **2004**, *14*, 3747; (f) Tan, Q.; Birzin, E. T.; Chan, W.; Yang, Y. T.; Pai, L.-Y.; Hayes, E. C.; DaSilva, C. A.; DiNinno, F.; Rohrer, S. P.; Schaeffer, J. M.; Hammond, M. L. *Bioorg. Med. Chem. Lett.* **2004**, *14*, 3753; (g) Blizzard, T. A.; DiNinno, F.; Morgan, J. D.; Wu, J. Y.; Chen, H. Y.; Kim, S.; Chan, W.; Birzin, E. T.; Yang, Y. T.; Pai, L.-Y.; Zhang, Z.; Hayes, E. C.; DaSilva, C. A.; Tang, W.; Rohrer, S. P.; Schaeffer, J. M.; Hammond, M. L. *Bioorg. Med. Chem. Lett.* **2004**, *14*, 3865; (h) Blizzard, T. A.; DiNinno, F.; Morgan, J. D.; Wu, J. Y.; Gude, C.; Kim, S.; Chan, W.; Birzin, E. T.; Yang, Y. T.; Pai, L.-Y.; Zhang, Z.; Hayes, E. C.; DaSilva, C. A.; Tang, W.; Rohrer, S. P.; Schaeffer, J. M.; Hammond, M. L. *Bioorg. Med. Chem. Lett.* **2004**, *14*, 3861; (i) Blizzard, T. A.; DiNinno, F.; Morgan, J. D.; Chen, H. Y.; Wu, J. Y.; Kim, S.; Chan, W.; Birzin, E. T.; Yang, Y. T.; Pai, L.-Y.; Fitzgerald, P. M. D.; Sharma, N.; Li, Y.; Zhang, Z.; Hayes, E. C.; DaSilva, C. A.; Tang, W.; Rohrer, S. P.; Schaeffer, J. M.; Hammond, M. L. *Bioorg. Med. Chem. Lett.* **2005**, *15*, 107.
3. Kamboj, V. P.; Ray, S.; Dhawan, B. N. *Drugs Today* **1992**, *28*, 227.
4. (a) Alexandersen, P.; Riis, B. J.; Stakkestad, J. A.; Delmas, P. D.; Christiansen, C. *J. Clin. Endocrinol. Metab.* **2001**, *86*, 755; (b) Bury, P. S.; Christiansen, L. B.; Jacobsen, P.; Jorgensen, A. S.; Kanstrup, A. K.; Naerum, L.; Bain, S.; Fledelius, C.; Gissel, B.; Hansen, B. S.; Korsgaard, N.; Thorpe, S. M.; Wassermann, K. *Bioorg. Med. Chem.* **2002**, *10*, 125.
5. Labrie, M.; Labrie, C.; Belanger, A.; Simard, J.; Giguere, V.; Tremblay, A.; Tremblay, G. J. *Ster. Biochem. Mol. Biol.* **2001**, *79*, 213.
6. Civelli, M.; Galbiati, E.; Caruso, G. P.; Amari, G.; Armani, E.; Ghirardi, S.; Delcanale, M. *World Congress of Pharmacology* **2002**, *24*: July 7–12 (Abs 96.19).
7. Grese, T. A.; Pennington, L. D. *Tetrahedron Lett.* **1995**, *36*, 8913.
8. For review of organotitanium chemistry, see: Reetz, M. T. In *Organometallics in Synthesis, A Manual*; Schlosser, M., Ed.; Organotitatnium Chemistry; John Wiley & Sons, 2002.
9. Blizzard, T. et al., in preparation.
10. Mitra, S. W.; Yudkovitz, J.; Fisher, P.; Tarachandani, A.; Wilkinson, H. A.; Hayes, E. C.; Boltz, D.; Rohrer, S. P.; Schaeffer, J. M. Abstracts, 26th San Antonio Breast Cancer Symposium, San Antonio, Texas, December, 2003.
11. Osborne, C. K.; Wakeling, A.; Nicholson, R. I. *Br. J. Cancer* **2004**, *90*(suppl 1), S2.
12. Rosati, R. L.; DaSilva Jardine, P.; Cameron, K. O.; Thompson, D. D.; Ke, H. Z.; Toler, S. M.; Brown, T. A.; Pan, L. C.; Ebbinghaus, C. F.; Reinhold, A. R.; Elliot, N. C.; Newhouse, B. N.; Tjoa, C. M.; Sweetnam, P. M.; Cole,

M. J.; Arriola, M. W.; Gauthier, J. W.; Crawford, D. T.; Nickerson, D. F.; Pirie, C. M.; Qi, H.; Simmons, H. A.; Tkalcevic, G. T. *J. Med. Chem.* **1998**, *41*, 2928.

13. The complexes of **4** and **3F** with the ligand binding domain of ER-alpha (residues 307–554) were crystallized by vapor diffusion, using a precipitant containing 100 mM $MgCl_2$, 6% PEG 3350, and 100 mM imidazole buffer, pH 7.1. Data for both complexes were measured at beamline 17-ID of the Advanced Photon Source. The crystals have the symmetry of space group $P6_522$, with cell dimensions $a = b = 58.55$, $c = 276.60$ (**4**) and $a = b = 58.85$, $c = 277.83$ (**3F**). The data were processed with program X-GEN, which yielded an R-merge of 0.085 for the data from ∞ to 1.9 Å (**4**) and an R-merge of 0.120 for the data from ∞ to 2.2 Å (**3F**). The structures were refined using program SHELXL, with final values for R-work and R-free of 0.190 and 0.258 for the data from 10.0 to 1.90 Å resolution (**4**) and 0.179 and 0.298 for the data from 10.0 to 2.20 Å (**3F**). Coordinates and structures factors for both complexes have been deposited with the Protein Data Bank (entries 1YIM and 1YIN). The structure of **I**, Z = S has been described previously (Ref. 2a; PDB ID 1SJ0).